Thermal Stress Relaxation and Creep Tests of Reinforced Concrete Beams Under Long Term Thermal Effects and Loadings

N. Shibasaki, H. Yoshida, Y. Sugawara
Nuclear Power Construction Dept., Tokyo Electric Power Co., Inc., 1-3, 1-chome, Uchisaiwai-cho, Chiyoda-ku, Tokyo 100, Japan

H. Itabashi, S. Furukawa
Tokyo Electric Power Service Co., Ltd., 3-1, 1-chome, Uchisaiwaicho, Chiyoda-ku, Tokyo 100, Japan

K. Okada, T. Mochida
Takenaka Technical Research Laboratory, Takenaka Komuten Co., Ltd., 5-14, 2-chome, Minamisuna, Koto-ku, Tokyo 136, Japan

ABSTRACT

It is well understood that the thermal stress of reinforced concrete members decreases; sometimes to a great extent, due to the development of cracks and/or creep of concrete. Although the long-term thermal effects must be considered in the structural design of a nuclear power plant of reinforced concrete or prestressed concrete, very few data were available. Hence, a series of tests of beams subjected to thermal gradient and external moment were conducted to obtain design guidelines for the long-term thermal effects.

Four beam specimens which had identical dimensions and reinforcement were provided for the test program. The beams were one-third the actual size. One specimen was subjected to a thermal gradient alone, while another one was subjected to the combined thermal gradient and sustained external moment. Test conditions were provided so as to reproduce actual loading condition during normal operating in a nuclear power plant. The other two, for creep tests, were used as reference specimens for the above two. The thermal gradient across the depth of a beam was provided by means of heating the bottom surface and, at the same time, exposing the top surface to the ambient temperatures in the testing room. To reproduce the thermal moment, a pure bending moment was applied so as to cancel out the curvature caused by the thermal gradient. Any change of curvature during the test period, about four months, was adjusted by controlling the moment so that the thermal curvature may be kept constant, zero. Thus, the reduction of the thermal moment was observed by measuring the change of the moment.

The following conclusions were obtained from this experiment.

1) The thermal moment decreased rapidly at an early loading stage when subjected to constant thermal gradient alone, because of the significant development of cracks and the occurrence of new cracks.

2) Independently of the existence of sustained external moment, the thermal moment reduced after two months loading to the calculated value based on the cracked section, effective Young's modulus and the creep coefficient φ_c as 1. This simple evaluation method was available to predict the reduction of the long-term thermal moment.

3) The estimated crack widths according to the CEB-FIP Model Code were considerably smaller than the test results at about 4 months loading. The long-term thermal effects such as creep of concrete at elevated temperature might have resulted in the considerably larger crack width than the estimated.

1. Introduction

It is well known that the thermal stress of reinforced concrete members decreases in accordance with the reduction of the stiffness caused by cracking and/or creep of concrete.

The thermal effects under short-term loading combined with, for example, earthquake force and the LOCA pressure have recently been well understood through a number of experimental studies[1]. The long-term thermal effects, however, have been still unknown due to the lack of sufficient test data. This often results in the difficulty to appropriately evaluate the thermal effects during the design for normal operating condition where the serviceability limit state governs the design. Therefore, it is strongly required to obtain the knowledge of time-dependent thermal effects under the occurrence and extension of cracks and/or the creep of concrete at elevated temperature.

From this background, an experimental program was undertaken for four reinforced concrete beam specimens so as to investigate the time-dependent thermal effects under the condition with or without external forces. Based on test results, the reduction of thermal moment and the development of cracks were mainly discussed in this paper. The application of the present available design method for the thermal effects was also discussed.

2. Experimental Program

2.1 Test Specimen: Walls and/or slabs of the fuel storage pool in a nuclear power plant were subjects of this study. Four reinforced concrete beams which represented a part of walls or slabs were provided for the test. The depth of the specimens were reduced to one-third the actual thickness of members. Overall dimensions and reinforcement details of each beam are given in Fig. 1. The length and the cross section of a specimen were 600cm and 30cm by 60cm, respectively. Mix proportion of concrete is shown in Table 2. Maximum size of coarse aggregate used was 20mm. Deformed bars of 29mm in diameter were used for main reinforcement. The yield strength and the ultimate strength were 3,980 kg/cm^2 and 6,010 kg/cm^2, respectively. And the reinforcement ratio was 0.71%. Two of these specimens were used for the thermal relaxation tests and the other two were for creep tests. Each surface of specimens except the exposed portion to ambient temperature was sealed with neoprene rubber sheets of 1mm thick to prevent water migration. The sealed condition was provided to reproduce the boundary conditions of members of actual plants covered by liners.

2.2 Experimental Program: The experimental program included the following two types of test;

(a) Thermal relaxation tests under the condition with or without the sustained external moment M_F.

(b) Creep tests under the conditions with or without thermal gradient ΔT across the depth of specimens.

The thermal relaxation tests were main subject in this research, and the creep tests were carried out as reference to estimate the time-dependent deflection of the main specimen due to the sustained external moment. Test types and load conditions were summarized in Table 1.

The thermal gradient of 40 deg. C and the temperature of 70°C at a heating surface were selected referring to the normal operating condition of nuclear power plants. The sustained external moment of 6.9 t.m was determined so that the design stress of reinforcement at the combined load condition may be arround the long-term allowable stress of 2,000 kg/cm^2.

2.3 Test Apparatus: Test apparatus to apply the thermal moment and the sustained external

moment are shown in Fig. 2. Each test specimen was set on roller and pin supports to allow free movement to longitudinal direction. The test span between the supports was 300cm.

The thermal gradient across the depth of a test specimen was produced by heating one side of the specimen (bottom surface) with a flexible electric panel heater attached to the surface. The surface temperature was kept constant at 70°C during the test period by a thermo-controller. The opposite surface (top surface) was exposed to ambient temperature in the testing room. To prevent heat issue from test portion, all the surfaces except the top surface were covered with plastic thermo-insulator of 100mm thick. The thermal moment, which cancels out the deflection induced by the thermal gradient, was applied with mechanical jacks provided at both ends of a specimen so that moment may be uniform in the test portion. The sustained external moment was applied and kept constant with springs through the test period.

2.4 Test Procedure

(a) Specimen RH-1 Subjected to the thermal gradient alone: After the specimen deflected because of the thermal gradient, the thermal moment to cancel out the curvature ϕT was applied. In this test, the curvature of test specimens was estimated from the measured displacement at the midspan using the relation given in eq.(1) with small errors.

$$\phi = (8/\ell^2)\cdot\delta m \qquad (1)$$

where ϕ : curvature of test portion, δm; displacement at midspan,
ℓ : length of the test portion.

The displacement at the midspan of the specimen was kept unchanged through the test period, canceling any changes of the displacement due to the reduction of stiffness and/or the temperature variation in the testing room by means of mechanical jacks.

(b) Specimen RH-2 at initial loading: Figure 3 shows the test sequence and the assesment of the thermal moment under the combined action with the external moment. This concept of the assesment was proposed by K. Irino et al.[2], and the test sequence was as follows.

After the specimen deflected due to the thermal gradient ΔT, the external moment M_F was applied. In that loading process, the curvature was assumed to change from $-\phi_T$ to ϕ_F, where ϕ_F is the curvature induced by M_F. The curvature before applying ΔT took zero in the figure. When an increment of some bending moment M_{T1} was subsequently applied, the curvature increased from ϕ_F to ϕ_1. The bending stiffness at that stage was estimated as the secant modulus, i.e., $(M_F + M_{T1})/(\phi_T + \phi_1)$, of the moment (M)-curvature (ϕ) diagram obtained during the test, considering the independency of the load sequence. In case that the bending stiffness decreased in that loading process, the curvature correspond to M_F increased from ϕ_F to ϕ_{F1}. Thus, the thermal moment M_T to cancel out the thermal curvature ϕ_T was obtained when the relation $\phi_1 - \phi_{F1} = \phi_T$ was satisfied in the incremental loading steps.

(c) Specimen RH-2 under long-term loading: External forces which act on structures under normal operating condition are normally unchanged and they may cause some additional deflections due to the time-dependent effects such as creep and/or the development of cracks. To investigate the long-term thermal effects under the combined external moment, the above mentioned long-term deflection must be separately considered from the total time-dependent deflection of the structure. To reproduce such loading condition, it is necessary to release the additional curvature caused by the action of M_F during the test period. To perform this procedure, the displacement at the midspan of the specimen was controlled by means of mechanical jacks so that any change of the displacement coincided with the additional displacement of the creep specimen MH-1, which was subjected to the same thermal gradient

and the external moment (see Fig. 4).

3. Test Results

3.1 Temperature Distribution and Variation through the Test Period: The temperature distribution of Specimen RH-1 in steady state was illustrated in Fig. 5. The temperature inside the test specimen was varied along the length due to the heat issue outside the test portion. Figure 6 shows the time-dependent variation of the temperature both inside the specimen and in the testing room through the test period. The thermal gradient was varied due to the daily variation in the room temperature and considerably decreased after two months.

3.2 Material Properties of Concrete: The observed thermal expansion coefficient α using sealed specimens (ϕ15 x 30cm) was 9.3 x 10^{-6}/°C as an average value. Mechanical properties both at the beginning and at the end of the experiment were shown in Table 3. Change of the compressive strength and the modulus of elasticity in the test period of time was merely 6.5% and 1%, respectively.

3.3 Initial Thermal Moment: The observed thermal curvature ϕT of both Specimens RH-1 and RH-2 due to the thermal gradient, approximately 40 deg. C, was 0.505 x 10^{-6}/mm. It was less than the calculated value 0.620 x 10^{-6}/mm, obtained from the eq.(2) where ΔT = 40 deg. C, α = 9.3 x 10^{-6}/°C and D was the depth of a specimen (D = 600mm).

$$\phi_T = \alpha \cdot \Delta T / D \qquad (2)$$

The inconsistency between these values was considered as a result of the variation of the temperature inside the specimen as shown in Fig. 5.

Figure 7 shows the observed moment-curvature relations. Initial thermal moment to cancel out the observed thermal curvature ϕ_T of Specimen RH-1 and RH-2 was 5.36 t.m and 2.94 t.m, respectively. The thermal moment of RH-2 decreased to 55% of that of RH-1 due to the decrease of the bending stiffness caused by the external moment.

3.4 Long-term Thermal Moment: Figure 8 shows the results of the relaxation test for Specimen RH-1 subjected to the thermal gradient alone. As indicated in the figure, the thermal moment decreased rapidly down to half the initial moment at the early stage of two or three weeks in the test period. The thermal moment continued to decrease, however, gradually thereafter.

Figure 9 shows the reduction of the thermal moment of Specimen RH-2 subjected to the same thermal gradient as RH-1 and the sustained external moment. The relaxation of the thermal moment at an early loading stage was considerably different from that of RH-1, since it decreased gradually through the test period.

Daily variation of the thermal moment and the remarkable shift after two months as seen in Fig. 8 and Fig. 9 were attributed to the variation of the thermal gradient as mentioned before (see Fig. 6).

3.5 Development of cracks: The observed crack widths and spacings of the test specimens both at the initial loading and after 131 days loading were shown in Table 5. The average crack spacing Am of Specimen RH-1 decreased from 27.3cm to 23.1cm because of the occurrence of new cracks during the test period. On the other hand, the average crack spacing of RH-2 remained little changed through the test period.

The observed average crack width Wm of Specimen RH-1 and RH-2 increased during the test period, from 0.046mm to 0.073mm and, from 0.163mm to 0.201mm, respectively. The increase of the crack width of RH-1 was more greater at the early loading stage of one month in the whole loading period. The increasing ratios of crack widths at the test end were 1.59 and 1.23 for RH-1 and RH-2, respectively.

4. Discussions on the Test Results

4.1 Reduction of Initial Thermal Moment: Table 4 shows the comparison of the experimental results and the calculated results. The initial thermal moment of both Specimens RH-1 and RH-2 were calculated for two types of the stiffness, i.e., (1) initial bending stiffness $(EI)_o$ obtained from the observed M-ϕ relation (the stiffness of the uncracked section), (2) the bending stiffness of the cracked section (EI)cr, neglecting the contribution of the concrete in tension between cracks. The initial thermal moment without the external moment, measured as 5.36 t.m, was about 75% of that calculated based on the stiffness of the uncracked section $(EI)_o$. The existence of the thermal cracks alone would have affected the reduction of the stiffness to a lesser extent.

The initial thermal moment under the combination with the external moment (M_F = 6.9 t.m) was measured as 2.94 t.m. It was about 40% of that calculated based on the stiffness $(EI)_o$, and was approximately equal to the calculated value based on the stiffness of the cracked section (EI)cr. The difference of the initial thermal moment between Specimen RH-1 and RH-2 was attributed to the application of the external moment M_F that caused the considerable development of cracks combined with the thermal moment.

4.2 Reduction of the Thermal Moment under Long-term loading: Figure 10 shows the test results compared with the calculated results regarding the reduction factor of the thermal moment, representing the loading period of time as log-scale. The factor was normalized by the stiffness of the uncracked section $(EI)_o$.

Although the factors of Specimen RH-1 and RH-2 at the early loading stage had been markedly different, they had come to close as the increase of the loading term, and coincided with each other after one month loading. The rapid reduction of the thermal moment of Specimen RH-1, which was subjected to the thermal gradient alone, at the early loading stage would have resulted from the significant development of crack width and the occurrence of new cracks during the period, as previously mentioned. While, the factor of RH-2 was scarcely changed during the test period. This was explained as follows. The bending stiffness of the specimen at the initial loading had been decreased approximately to the value based on the stiffness of the cracked section, thus the reduction of the stiffness due to the time-dependent development of cracks had been very few.

4.3 Calculation of the Long-term Thermal Moment: As was indicatee in Fig. 10, the reduction factors of the thermal moment of both Specimens RH-1 and RH-2 decreased, after one month loading, to the calculated value based on the stiffness of the cracked section (the effect of creep was not accounted). And they further decreased gradually with time under load due to the time-dependent effects. To take into account of the effect of creep, the effective Young's modulus Ee, given in eq.(3), was employed instead of the modulus of elasticity Ec in the calculation of the stiffness of the cracked section.

$$Ee = Ec/(1 + \varphi_c) \qquad (3)$$

where φ_c is the creep coefficient of concrete.

The calculated results, when φ_c took 1, were shown in Table 4 and also in Fig. 10 compared with the test results. From these comparisons, it was concluded that the reduction factor under two months loading coincided the calculated value when φ_c took 1. In addition, the decreasing tendency of the observed reduction factor suggested that the thermal moment would be finally decreased to the calculated values for φ_c equal to 2 or 3.

4.4 Crack Widths and Spacings: The comparison of the observed crack widths and the spacings

with the calculated results according to the CEB-FIP Model Code [3] was shown in Table 5. The calculated crack spacings agreed fairly well with the test results except those of RH-1 at the initial loading, however, the calculated value of the crack widths considerably underestimated the test results. One of the reasons of the discrepancy between test and calculated results would be that the long-term thermal effects on the crack widths, such as creep of concrete at elevated temperature, were not included in the Model Code.

5. Conclusions

1) The thermal moment decreased rapidly at an early loading stage when subjected to constant thermal gradient alone, because of the significant development of cracks and the occurrence of new cracks.

2) Independently of the existence of sustained external moment, tbe thermal moment reduced after two months loading to the calculated value based on the cracked section, effective Young's modulus and the creep coefficient φ_c as 1. This simple evaluation method was available to predict the reduction of the long-term thermal moment.

3) The estimated crack widths according to the CEB-FIP Model Code were considerably smaller than the test results at about 4 months loading. The long-term thermal effects such as creep of concrete at elevated temperature might have resulted in the considerably larger crack width than the estimated.

References

[1] Y. Ohsaki et al., "Drafted Japanese Design Criteria for Concrete Containment", 6th SMIRT Conference Paris, France (1981).

[2] K. Irino et al., "An Experimental Study on Thermal Stress of Reinforced Concrete Members under Short-term Loading", 7th SMIRT Conference Chicago, USA (1983).

[3] International System of Unified Standard Codes of Practice for Structures, CEB-FIP Model Code for Concrete Structures, 3rd Edition 1978.

Table 1. Test type and load condition

Test specimen	Test type	ΔT (deg. C)	M_F (t.m)	Ti (°C)
RH-1	Relaxation	40	0	70
RH-2	Relaxation	40	6.9	70
MH-1	Creep	40	6.9	70
MC-1	Creep	0	6.9	-

where ΔT : thermal gradient across the depth of beams
M_F : external moment
Ti : temperature at heated surface

Table 2. Mix proportion

W/C (%)	S/A (%)	Water (kg/m^3)	Cement (kg/m^3)	Fine aggregate (kg/m^3)	Coarse aggregate (kg/m^3)	Slump (cm)	Air (%)
58	44.2	163	281	814	1,047	12	6

Table 3. Mechanical properties of concrete

Test item \ Age	At the beginning of experiment (59-days)	At the end of experiment (166-days)
Compressive strength (kg/cm^2)	368	392
Tensile strength (kg/cm^2)	27.1	-
Modulus of elasticity (kg/cm^2)	3.09×10^5	3.12×10^5

Table 4. Test and calculated results of thermal moment (Unit: t.m)

	Initial loading				Two months after		
	Test result	Calculated value (1)	Calculated value (2)	Reduction factor	Test result	Calculated value (3)	Reduction factor
RH-1	5.36	7.13	2.46	0.75	2.16	2.19	0.30
RH-2	2.94	7.37	2.48	0.40	2.22	2.21	0.30

Calculated value (1) : was based on the stiffness of the uncracked section $(EI)_o$

Calculated value (2) : was based on the stiffness of the cracked section $(EI)_{cr}$, neglecting the contribution of concrete in tension between cracks

Calculated value (3) : was based on the stiffness of the cracked section using the effective Young's modulus (creep coefficient φ_c taken 1).

Reduction factor was defined as the ratio of the measured thermal moment to the calculated value (1).

Table 5. Crack widths and spacings

Test specimen	Initial Loading				131-days after			
	Am (cm)		Wm (mm)		Am (cm)		Wm (mm)	
	Test result	Calculated value	Test result	Calculated value	Test result	Calculated value	Test result	Calculated value
RH-1	27.3	23.3	0.046	-	23.1	23.3	0.073	0.056
RH-2	21.4	23.3	0.163	0.129	20.0	23.3	0.201	0.153

where Am : mean crack spacing
Wm : mean crack width

Calculated values were according to CEB-FIP Model Code

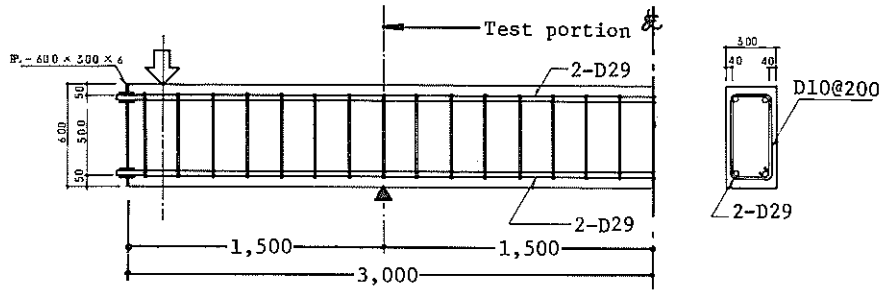

Fig. 1 Test sepcimens

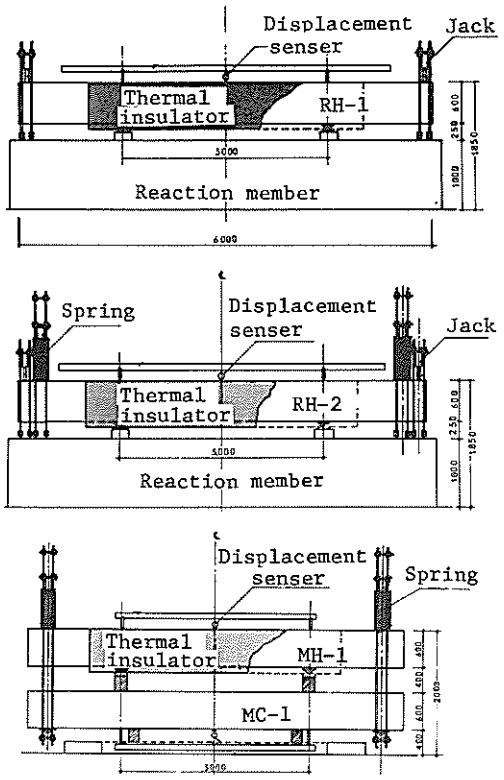

Fig. 2 Test apparatus

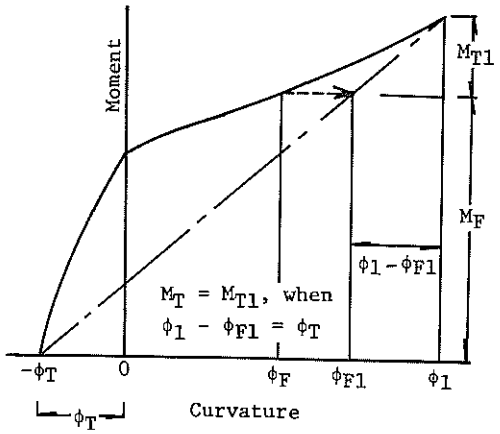

Fig. 3 Test sequence at initial loading

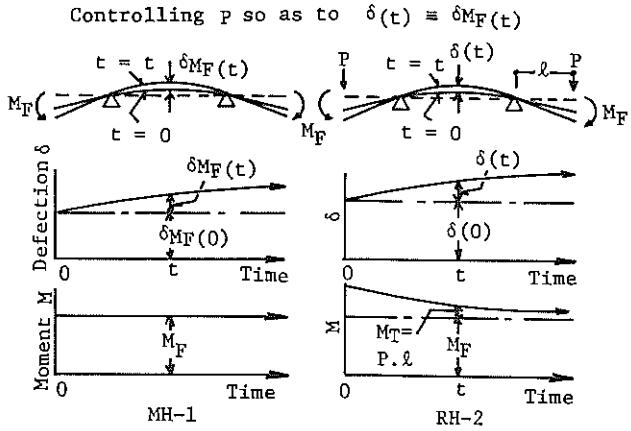

Fig. 4 Test procedure under long-term loading

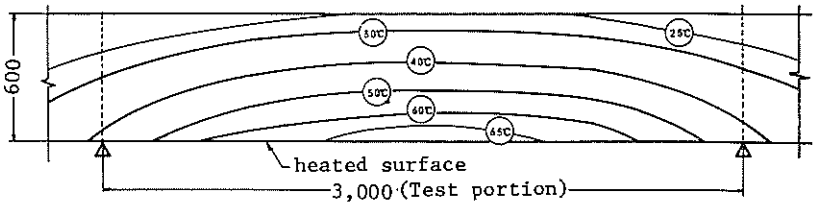

Fig. 5 Temperature distribution inside the specimen

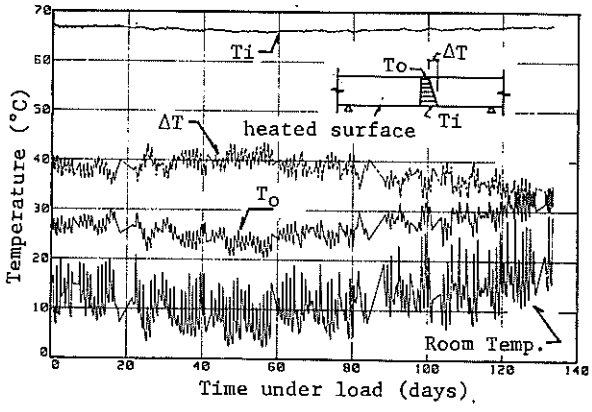

Fig. 6 Time-dependent variation of temperature

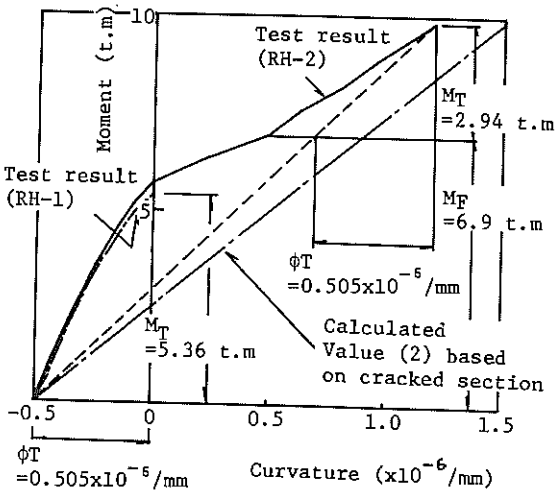

Fig. 7 Applied moment-curvature relation at the initial loading

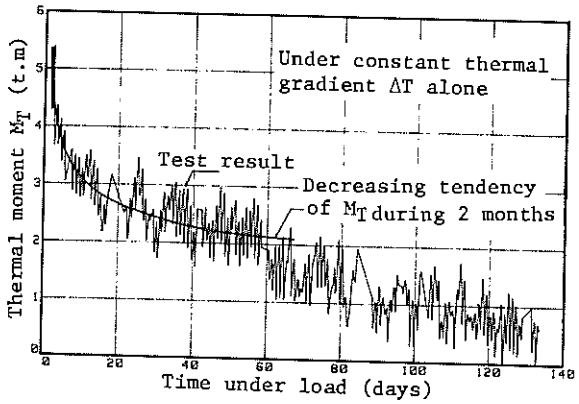

Fig. 8 Variation of thermal moment during the test period (RH-1)

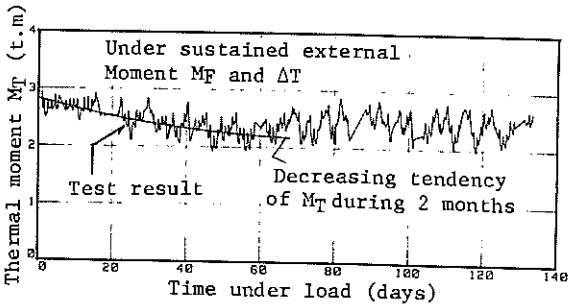

Fig. 9 Variation of thermal moment during the test period (RH-2)

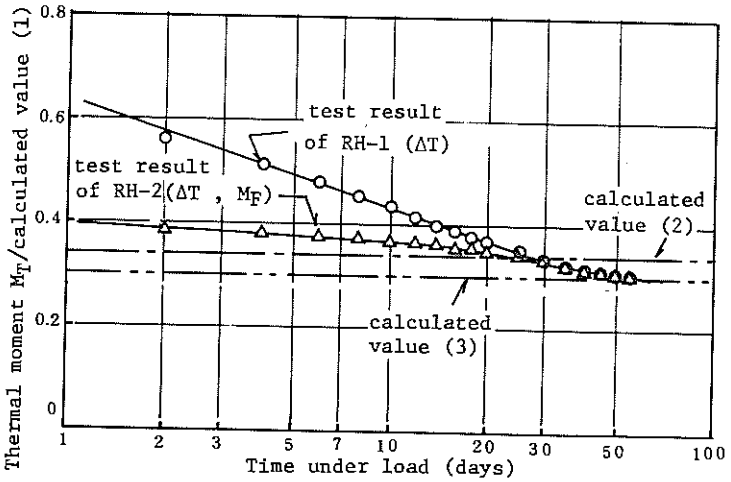

Calculated value
(1) based on uncracked section
(2) based on cracked section
(3) using effective Young's modulus Ee=Ec/(1 +φc), where φc taken 1

Fig. 10 Comparison of test results and calculated thermal moment